April 2008

Electrospinning Organometallics to Produce Metallic Fibers

Brendan F. Malloy
Worcester Polytechnic Institute

Project Number: SYS - 2007

Electrospinning Organometallics to Produce Metallic Fibers

A Major Qualifying Project Report

Submitted to the Faculty

of the

WORCESTER POLYTECHNIC INSTITUTE

in partial fulfillment of the requirements for the

Degree of Bachelor of Science

in Mechanical Engineering

by

Brendan Malloy

_____

Date: April 2008

Approved:

_____

Prof. Satya Shivkumar, Major Advisor

Table of Contents

Abstract

The goal of this project was to fabricate nanowires by electrospinning an organometallic solution and burning off the organic component of the compound. The degradation properties of the organometallic were observed by direct heating in a furnace, differential scanning calorimetry, x-ray diffraction and energy dispersive spectroscopy. Several different solutions were electrospun resulting in the formation of both fibrous meshes and spray coatings. Solutions containing a polymer displayed significant improvement in viscoelastic properties, resulting in improved electrospinnability. After thermal degradation, EDS analysis confirmed the presence of tin and tin oxide structures. The addition of binding agents could facilitate the formation of more complex tin microstructures.

1. Introduction

The field of nanotechnology has existed ever since the invention of the first electronic devices. The promise of applying nanotechnology to medical treatment and the scaling down of electronics, along with general miniaturization, has lead to a boom in the development of this rapidly growing field [1]. The simple act of changing the size of a structure can have profound effects on physical properties such as melting point, electrical conductivity, and magnetic properties [1]. Material purity maximizes due to the inherent lack of defects when working at such small scales. These new properties can lead to more diverse applications. The ability to apply existing technology to the development of nanomaterials could significantly facilitate research. One such technology whose application could be expanded is electrospinning.

Electrospinning has already been used for years to produce polymer nanofibers [1-4]. If electrospinning could be utilized to fabricate metallic fibers, completely new materials possessing unique physical structures and properties could be produced. These materials could see a variety of applications in their stand-alone form, such as filtration, or they could be incorporated into composite materials. This study investigated the fabrication of metal/metal-oxide fibers by means of electrospinning an organometallic compound. The degradation properties of the chosen organometallic were analyzed by thermally degrading the compound in a furnace, differential scanning calorimeter, x-ray diffraction and energy-dispersive spectroscopy. The structures formed by electrospinning different organometallic solutions were analyzed using a scanning electron microscope.

2. Background

2.1 Uses of Metallic Fibrous Structures

Metal bars and fibers have been used for decades to imbue existing materials with superior mechanical properties. Steel rebar can be seen in use every day to reinforce concrete structures. This same concept is applied, albeit at a much smaller scale, when metal and ceramic fibers are used as composite matrices in the fabrication of metal parts. These metal matrix composites can significantly improve frictional properties, wear resistance, strength and thermal diffusivity [5-7].

Modern disc-brakes are composed primarily of cast iron or ceramic. Steel fibers are incorporated into the cast to form a composite that offers much higher wear resistance [7]. However, these steel fibers can result in aggressive warping of the disc due to the high heats generated. Copper and aluminum fibers are often added to improve thermal diffusivity and maintain the coefficient of friction at high temperatures.

Other metal and ceramic fibers have been used to form composite materials for use in other parts of automobiles such as engine blocks, pistons, cylinder liners and driveshaft [5,6]. Table 1 shows a variety of potential applications of metal and ceramic fiber composites.

Table i - Selected Potential Applications of Cast Metal Matrix Composites [5]

Composite	Application	Special Features
Gr / Al	Bearings	Cheaper, lighter, self-lubricating; conserves Cu, Pb, Sn, Zn, etc.
Gr/Al, SiC-Al2O3/Al fiber, Al/FP	Automobile Pistons, cylinder liners, piston rings, connecting rods	Reduced wear, anti-seizing, cold start, lighter, conserves fuel, improves efficiency
Gr / Cu	Sliding electrical contacts	Excellent conductivity and anti seizing properties
SiC / Al	Turbocharger impellers	High temperature use
Glass or Carbon bubbles in Al		Ultralight materials
Cast Carbon / Mg Fiber Composites	Tubular composites for space structures	Zero thermal expansion, high temperature strength, good specific strength and stiffness
Zircon/Al, SiC/Al, SiO2/Al	Cutting tools, machine shrouds, impellers	Hard, abrasion resistant materials
Al-char, Al-clay	Low cost, low energy materials	

The fabrication of micro- and nano-fibers can result in the formation of porous structures. These structures exhibit high surface area which can be utilized for use as heat exchangers [8]. L. Tadrist et al. [8] have found that these porous structures possess unique characteristics leading to strong thermal performance. The use of a metallic matrix showed higher heat transfer than standard heat fins.

The porous nature of fibrous structures can also be utilized for filtration. Fibrous bed filtration has been found to be an effective and efficient method for removing fine dust from gas flows [9]. Filters composed of metallic fibers are desirable for use in high temperature environments. Also, while standard flat filters use surface filtration to stop particles, a fibrous bed can catch particles on the surface and inside the body of the filter. Very fine particles that would otherwise travel through the filter can be captured by electrostatic forces generated by the metal.

2.2 Production of Fibrous Structures

Large diameter metal fibers such as rebar are produced by pouring molten metal in to casts. Smaller diameter metal fibers are typically fabricated by wire drawing. In this process, a cylindrically shaped piece of stock metal is pulled through a die, reducing the cross-sectional area. The sample is drawn through successively smaller dies until the desired fiber diameter is reached [10].

Powder metallurgy (P/M) offers a method of part fabrication that allows the porosity to be controlled. Metal powders are produced through a variety of methods including atomization, reduction, and electrolytic deposition. These powders are pressed into a mold of the desired part, forming a green compact. The size and shape of the powder particles, combined with the pressured applied in the mold, dictate the density and porosity of the final part [10]. The compact is then sintered at a temperature lower than the melting point, but high enough to allow bonding, resulting in the formation of the final part.

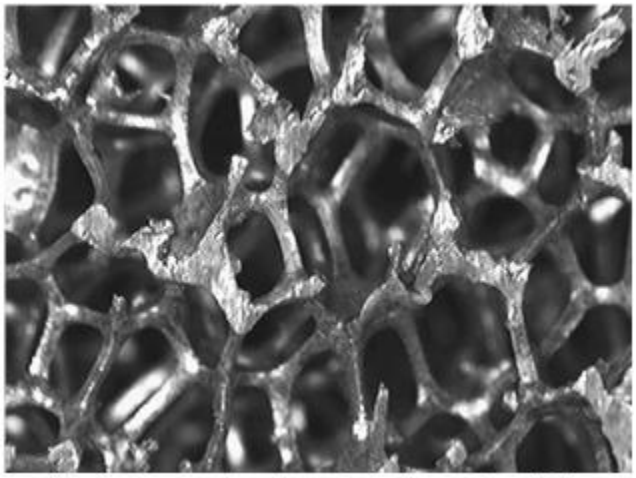

Fig. 1 - Porous structure of aluminum foam [8]

A newer method for producing porous, metal fiber structures, like those shown in Figure 1, is metal foam. The foams are made by combining an alloy, usually aluminum or zinc, with a titanium or zirconium hydride, which results in a uniform, foam-like substance [11]. This material is typically used for absorbing shock impacts

without elastic rebounds and can be used as a substitute in some metal parts in order to reduce weight.

2.2.1 Novel Methods for Producing Fibers

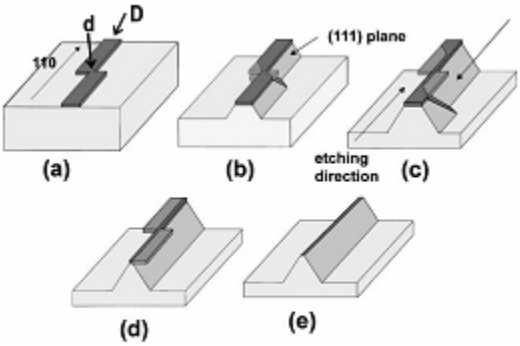

Fig. 2a-e. EBL and etching techniques leading to the formation of a reverse V-groove nanowire [12]

In the pursuit of producing fibers on increasingly smaller scales, several unique methods of micro- and nanowire fabrication have been developed. Figure 2 shows an example of one such method. Electron beam lithography is a standard technique used for nanometer scale patterning [12]. During this process, EBL is used to produce a mask, ~90nm wide, on the surface of an Si or SiGe substrate. Anisotropic wet etching is then used to remove layers of the underlying substrate along the (111) direction. The area under the mask is then etched, forming an inverted V-groove shaped wire. Wires as small as 60nm have been produced using this method.

Another method utilizing a similar etching process has also been developed to produce Si/SiGe nanowires [12]. A thin aluminum film is sputter coated on the surface of a Si/SiGe substrate. By operating an atomic force microscope (AFM) in "contact-mode" with a silicon probe, oxidation can be controlled to form patterns on a metallic

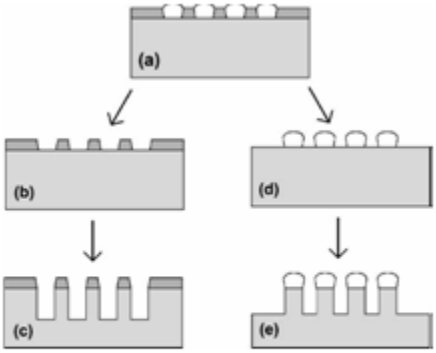

Fig. 3. Etching process using oxidized aluminum film. (b)-(c) remove oxide and underlying substrate. (d)-(e) remove aluminum and underlying substrate [12]

sample. Using appropriate voltage and scanning rates, aluminum oxide lines are patterned on the surface of the substrate. Increasing voltage increased the depth of oxidation. Chemical etching can then be applied to remove either the oxide lines or the remaining aluminum film. Further etching removes the underlying substrate forming Si/SiGe nanowires as small as 60nm. An outline of this process is shown in Figure 3.

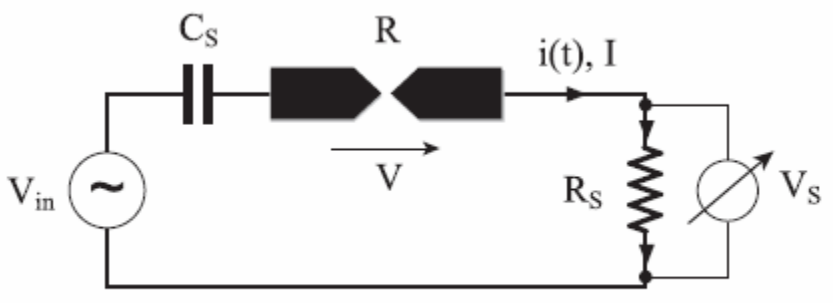

Fig. 4. Schematic of the circuit used for Au partical trapping [13]

Figure 4 shows a radically different approach to nanowire fabrication [13]. Two gold (Au) electrodes were fabricated on a silicon substrate using EBL techniques. The gap between the electrode tips was on the sub-micrometer range (20-500nm). A solution containing Au nanoparticles of diameters ranging from 10-100nm was also prepared. By applying appropriate AC voltages, Au nanoparticles were trapped between the electrodes and fused together, forming particle chains or nanowires depending upon the series impedance. Using this method allows control over both the diameter and width of the nanostructures produced. SEM photographs of the process are shown in figure 5.

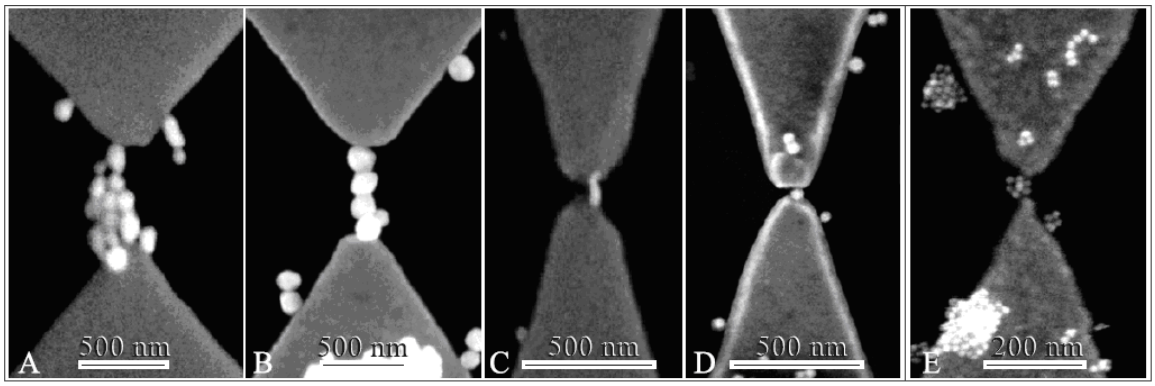

Fig. 5. SEM photographs of Au particle trapping. (A) and (B) show chains formed by large nanoparticles. (C) shows a wire formed by small nanoparticles. (D) shows a single small nanoparticle and (E) shows a cluster of small nanoparticles [13].

Nanowires have also been successfully produced using a process analogous to casting [14]. Pores were formed in a 99% pure aluminum substrate by treatment in phosphoric acid. The average pore diameter and length was 200nm and 50μm, respectively. The substrate was then placed in a zirconia-based sol-gel, causing the sol to fill the pores. Excess sol-gel was removed by polishing after the substrate had dried. Figure 6 shows the resulting nanowires.

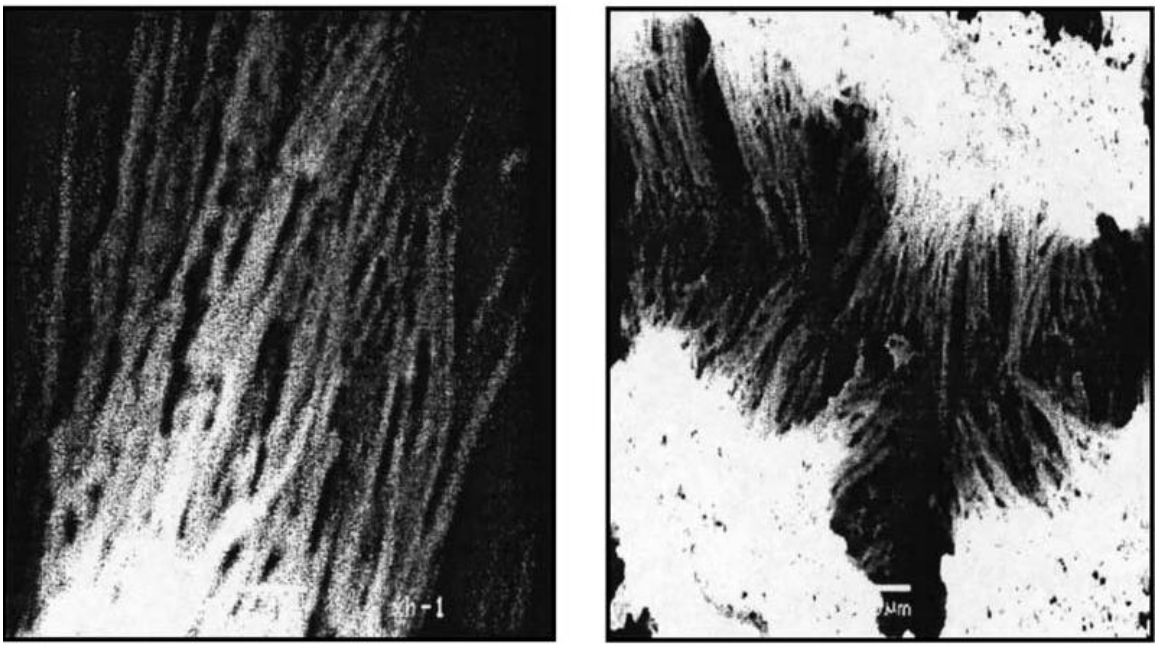

Fig. 6. Zirconia nanofibers produced by the sol-gel technique [14].

H. Y. Dang et al. [15] show an incredibly simple and equally effective method of producing metal oxide nanofibers by heating metal powder. Zinc powder was placed in a quartz tube and placed in a tube furnace. A protective argon atmosphere was provided until the sample was heated to just above its melting point, upon which time and 20% oxygen and 80% argon atmosphere was substituted. The resulting fibers, shown in Figure 7, were collected from the surface of the original powder sample.

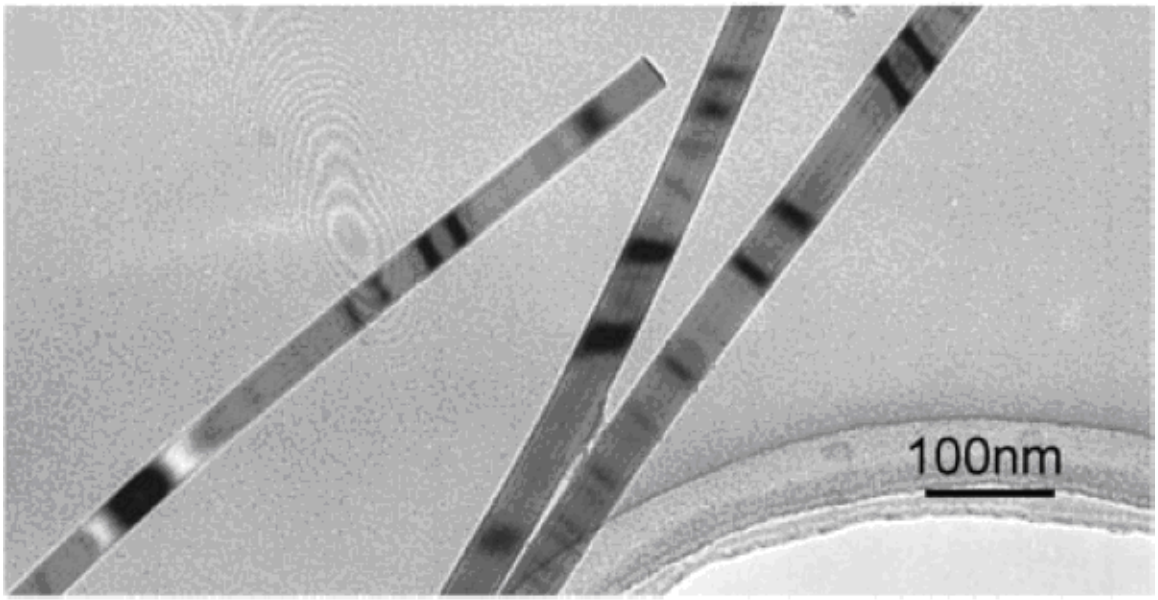

Fig. 7. TEM image of ZnO nanowires [15].

The fibers were single crystals of uniform structure with an average diameter of 40nm and were up to tens of micrometers long. This process also worked when used on magnesium and germanium powders.

2.2.2 Electrospinning

Electrospinning is a long existing technology originally developed for the fabrication of ultrathin, continuous, non-woven polymer fibers [1-4]. Figure 8 shows a typical electrospinning apparatus.

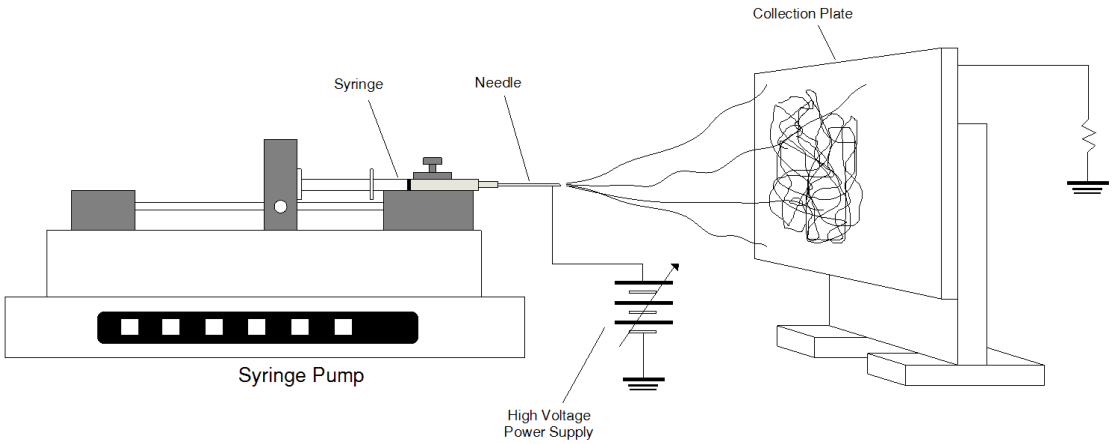

Fig. 8. Schematic of an electrospinning apparatus

During the process, a high voltage source inputs and charge on the tip of a needle/spinneret containing a polymer solution or melt. The difference in polarity between the solution and the grounded collection plate cause electrostatic forces. When these forces overcome the surface tension of the solution/melt in the needle, a polymer fiber is ejected. While the fiber travels from needle to the collection plate, much of the solvent evaporates [2]. The fiber also elongates, causing the diameter to shrink, due to unstable electrical forces causing the jet to bend, whip and split during transit [4]. By the time the fibers collect on the plate, their diameter thins to the micro- and nanometer range. Over 30 polymers have been successfully

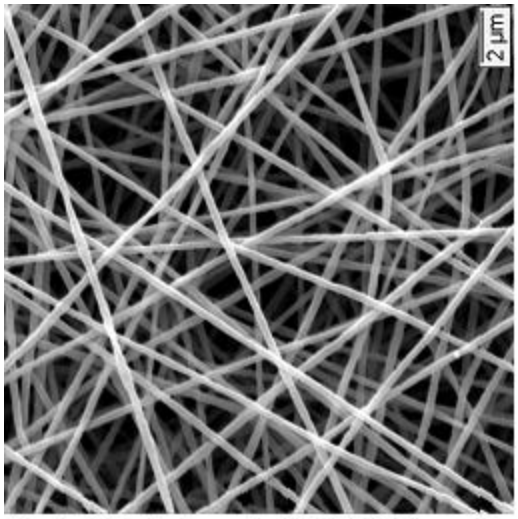

Fig. 9. SEM photograph of 20.2% PS fibers [4]

electrospun, producing fibers on the range of 40-500nm [1]. Figure 9 shows the fibers resulting from the successful electrospinning of a polystyrene solution. Applications of electrospun fibers include scaffolding for tissue engineering, drug delivery, filtration, protective clothing, and wound dressings.

2.2.3 Organometallics

An organometallic compound is defined as chemical compound where a metal is covalently bonded to carbon, although exceptions do exist [16]. While wide spread use of these compounds is limited because of toxicity, they are very useful when applied as catalysts. Organotins in particular are commonly used for polymer-stabilization and as polymerization catalysts as well as for biocidal applications (destroying microorganisms, insects, and plants) [17,18]. Organometallics are also soluble in most organic solvents, which is why this project is investigating their use in electrospinning. This solubility provides a simple and interesting method for getting a metal into solution.

2.2.4 Electrospinning of Metallic Fibers

The successful synthesis of tin oxide (SnO2) fibers by electrospinning has been published by Wang et al [19]. The research group made a tin oxide sol-gel from anhydrous tin (IV) chloriline (SnCl4). The sol-gel was mixed with poly(ethylene oxide) (Mw 900,000) and chloroform to form a homogeneous precursor solution. Thermal decomposition produced SnO2 fibers with diameters ranging from 100nm to

several micrometers. Figure 10 shows a single fiber before and after sintering at 600 C.

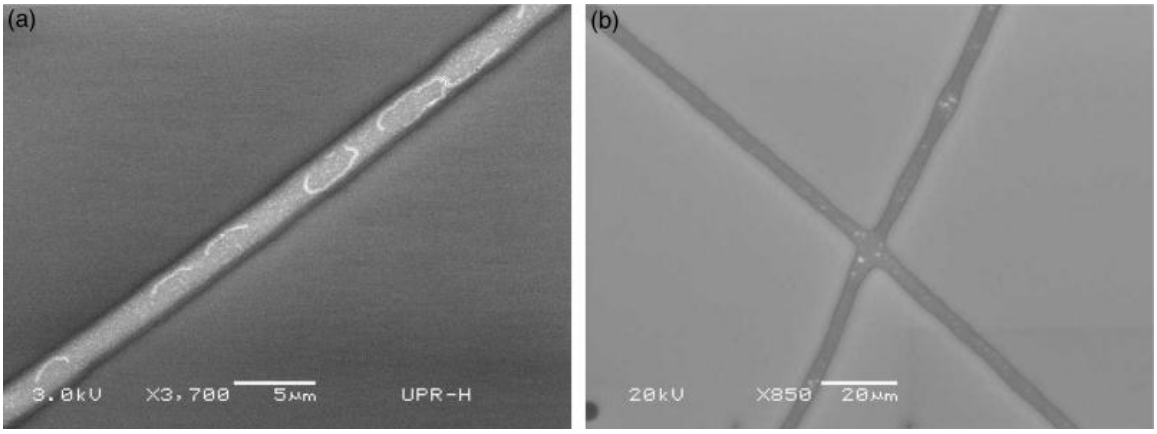

Fig. 10. SEM photographs of a single fiber before sintering (a) and after sintering (b) [19].

Porous anatase titania nanofibers have also been successfully produced by electrospinning an ethanol solution containing titanium tetraisopropoxide and poly(vinyl pyrrolidone) (PVP) [1].

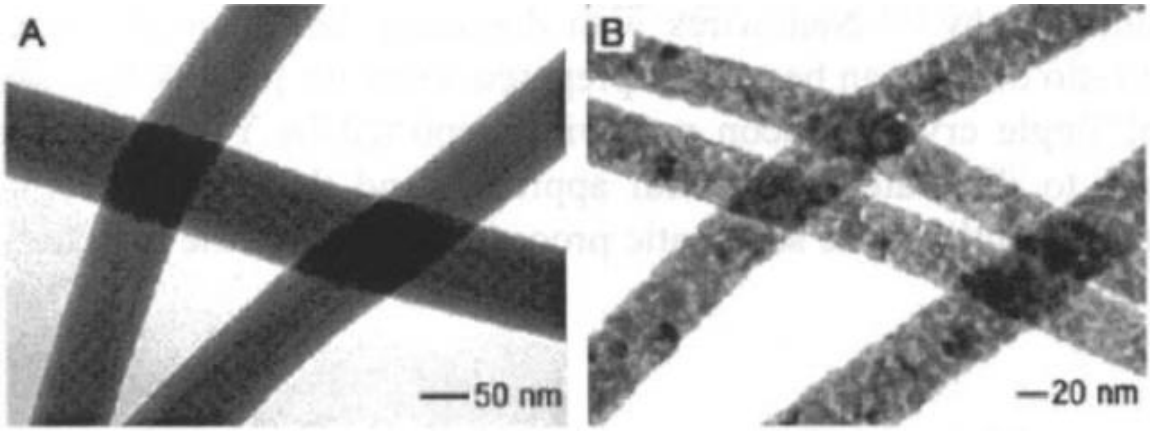

Fig. 11. (A) TEM of TiO2/PVP composite nanofibers. (B) same fibers after being degraded [1].

Figure 11 shows the resulting PVP/TiO2 composite nanofibers that formed as well as the porous TiO2 fibers that remained after pyrolysis of the PVP at 500 C.

3. Objectives

- To identify a suitable organometallic for use in producing metal or metal oxide fibers
- To examine the thermal degradation characteristics of the chosen organometallic
- To electrospin the chosen organometallic and analyze the structures formed
- To thermally degrade the electrospun structures to form metal or metal oxide fibers
- To examine the feasibility of producing nano-alloy fibers by mixing organometallics

4. Experimental Design

Figure 12 shows the experimental design used in this study.

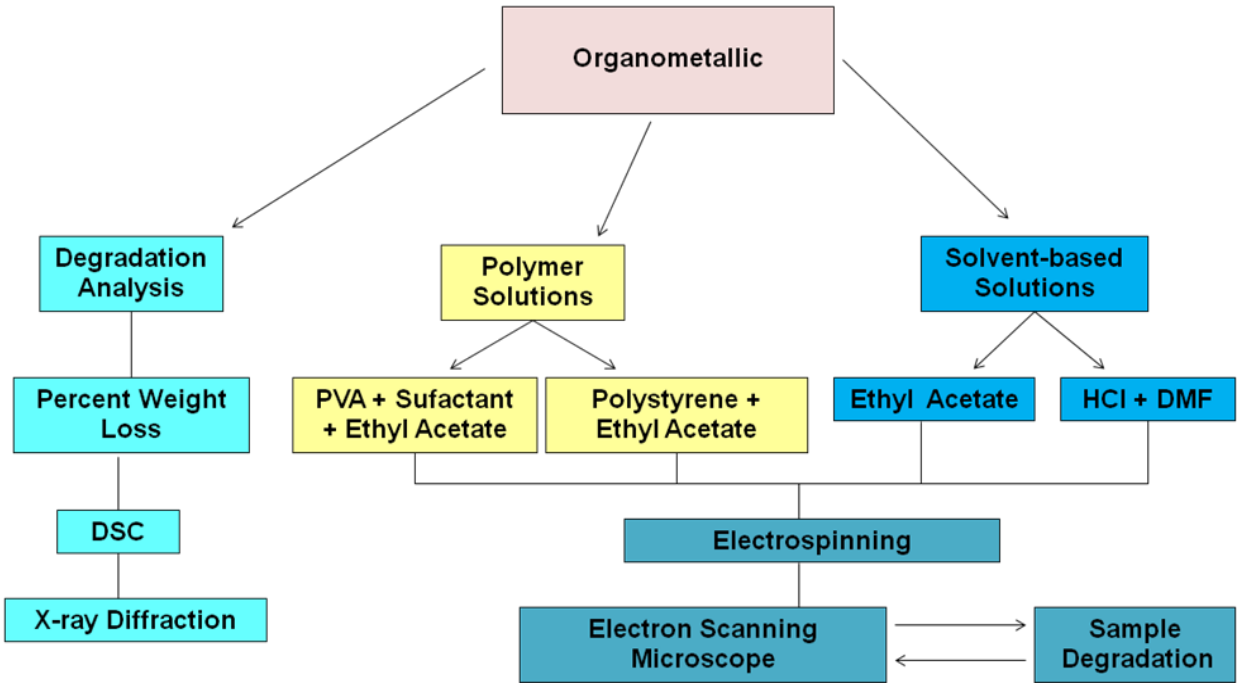

Fig. 12. Outline of experimental design.

Choosing the organometallic that was used in this study was one of the most important choices made during the development of this project. The criteria used for the

selection of the material were melting point, molecular structure and price. A melting point between 100 C and 350 C was considered most desirable as this range was relatively low, making the material easier to handle and test, but high enough that the degradation temperature was higher than those of the polymers that would be used in several of the solutions. The molecular structure of the material can have a significant effect on the properties of the material. Tetraphenyllead, an organometallic considered for use in this study, has the molecular structure shown in figure 13.

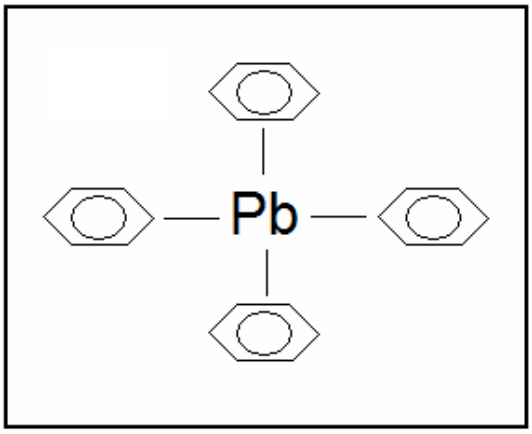

Fig. 13. Molecular structure of tetraphenyllead.

This organometallic's melting point is 227 C, well within the chosen range. However, the four phenyl rings surrounding the lead atom make this particular compound undesirable. The bond formed by a phenyl ring is very strong and can require significant heating above the material's melting point before degradation begins. Organometallics without these types of structures were given preference during the selection process. Price became the most limiting variable in the selection of the organometallic as the project budget was small and these types of materials can be very expensive. After considering all these criteria, a purchase of butyltin chloride dihydroxide was made from Sigma-Aldrich Co. This organotin was the

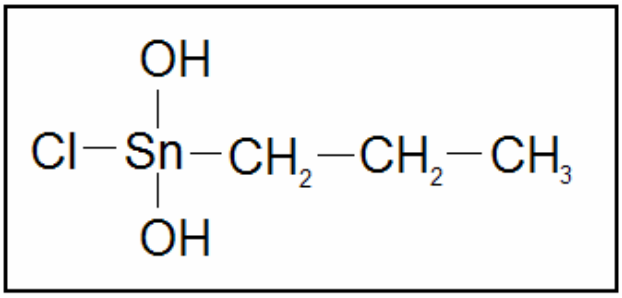

Fig. 14. Molecular structure of butyltin chloride dihydroxide

best valued organometallic available at $34 for 100g, had a melting point of 150 C and had an acceptable molecular structure.

The preliminary method used to investigate the degradation of the organometallic compound was to heat the powder in a furnace. This provided two important pieces of information. First, the physical reaction of the material to thermal degradation could be observed. If the organometallic reacted violently when heat was applied, then it would be unlikely that any structure formed after electrospinning would survive the degradation step that followed. This test also measured the total weight loss of the compound when held at a constant temperature. The temperatures chosen for this test reflected the known properties of the organometallic being used. Butyltin chloride dihydroxide had a melting temperature of 150 C and the base metal of the compound, tin, had a melting point of 231 C. 200 C was the chosen starting temperature as it seemed sufficiently high to cause degradation while also staying under the melting point of the tin. Exceeding the melting temperature of the base metal could accelerate oxidation or cause the metal itself to degrade, which could affect the results. Data were also collected above tin's melting point at 250 C, 300 C, 400 C, 500 C and 600 C.

Fig. 15. Perkin Elmer Differential Scanning Calorimeter.

A differential scanning calorimeter (Perkin Elmer DSC 7, Figure 16) was used to verify data gathered from the above degradation analysis. The sample in the DSC is heated linearly over a range of temperatures and the

amount of heat necessary to increase the temperature of the sample is recorded. The resulting model can show phase transitions, which are important to understanding the behavior of the organometallic under heating. The model generated by this scan was used in conjunction with the previously gathered data to choose the temperature at which the electrospun samples were degraded.

Other important methods for examining the degradation of the organometallic were x-ray diffraction (XRD) and Energy-dispersive x-ray spectroscopy (EDS). By utilizing these tests, the product of the degraded organometallic powder and electrospun fibers could be identified.

In order to investigate the electrospinnability of the organometallic compound, two types of solutions were tested. One solution was polymer based and the other solution was primarily composed of organic solvent. Electrospinning a solution containing both a polymer and the organometallic seemed appropriate as the use of polymer solutions in this process has been done for decades with well documented success. The polymer was intended to spin into a fibrous mesh and, if the organometallic is sufficiently dissolved, hold the organotin powder in the shape of a fiber. From here, the polymer and organic component of the organometallic would be burned off, ideally leaving behind a metal and/or a metal oxide strand.

Introducing extra additives such as polymers to a solution can result in complications. The polymer must be soluble in the same solvent as the organometallic

and the polymer must also degrade at a sufficiently low temperature so as to not influence the intended degradation temperature. Polymers could also leave carbon residues upon degradation, which would inhibit the ability to determine results of an electrospinning trial. To negate this possibility, solutions composed only of the organometallic and an appropriate solvent were also tested. However, not containing a polymer can lack sufficient viscosity to be effectively electrospun, resulting in the liquid spraying out of the needle instead of being extruded as a fiber.

Samples obtained by electrospinning both types of solutions were analyzed by scanning electron microscope (SEM). This analysis helped realize the electrospinnability of each type of solution. The samples were then thermally degraded and analyzed again in the SEM in order to observe whether or not metal or metal oxide fibers had been successfully produced.

5. Methodology

5.1 Degradation Analysis

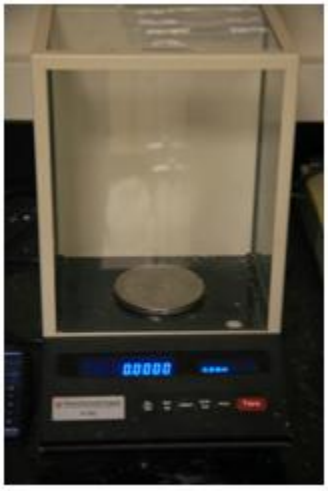

Fig. 16. DIC A-250 Scale

Aluminum foil was molded into small cups and their initial mass was measured on a scale (Denver Instrument Company, A-250. See Figure 16). Butyltin chloride dihydroxide powder (96% purity) was placed in a cup and the mass was measured again in order to determine the initial mass of the sample. The cup was the inserted into a furnace (Thermolyne 47900, Figure 17) set at 200 C. The sample was heated for five minutes increments before being removed and

allowed to cool. Placing the sample on the scale while it was still hot produced an unstable measurement. The sample was heated, cooled and measured until no discernable change in mass could be determined. This test was repeated for furnace temperatures of 175 C, 250 C, 300 C, 400 C, 500 C, and 600 C. During this process, the behavior of the compound during heating was observed and the percent weight loss over time was calculated.

Fig. 17. Thermolyne 47900 Furnace

DSC analysis was performed by preparing 3.1mg and 3.3 mg samples of organotin powder in small aluminum specimen holders. A temperature range of 15 C to 450 C was selected. Heating was set to take place at 10 C per minute and the DSC was left to complete the scan.

Degradation analysis was completed by performing x-ray diffraction. A sample of the degraded powder from the weight loss test was placed into an aluminum holder and secured into the XRD machine. The sample was set to run from 20 to 150 degrees. The scan took approximately 30 minutes to complete.

5.2 Electrospinning

For the electrospinning stage of the experiment, several solutions, shown in Table 2 were prepared.

Table ii - Solutions used for electrospinning trials

Solution						
1	2	3	4	5	6	7
1g Polyvinyl Acetate 2g SDS (Surfactant) 0.5g Organotin 12g Distilled Water	0.08g Polystyrene 0.02g Organotin 1mL Ethyl Acetate	0.005g Organotin 1mL Ethyl Acetate	0.02g Organotin 0.4mL HCl 0.5mL Ethanol	0.12g Polystyrene 0.02 Organotin 1mL Ethyl Acetate	0.05g Organotin 1mL Ethyl Acetate	0.2g Organotin 0.2mL HCl 1mL DMF

Each of the solutions were placed into syringes equipped with 30 gauge needles, except for solution 1 which was also electrospun using an 18 gauge needle. For each run, a syringe was mounted horizontally on a syringe pump (EW-74900-00, Cole-Parmer) that was calibrated to achieve a flow rate of 1mL/hr. The high voltage power supply was set to 10kV and the collection plate was placed 10cm from the tip of the needle for all experiments. Each electrospinning session took place at room temperature (68-74 F) and between 23% and 27% humidity. The needle tip and collection plate were both contained within a plexiglas chamber for the entirety of each electrospinning run. Each of the resulting samples were left to dry for at least twelve hours before being cut into segments for analysis in the scanning electron microscope or degradation in the furnace at 300 C. The electrospinning apparatus used is show in Figure 18.

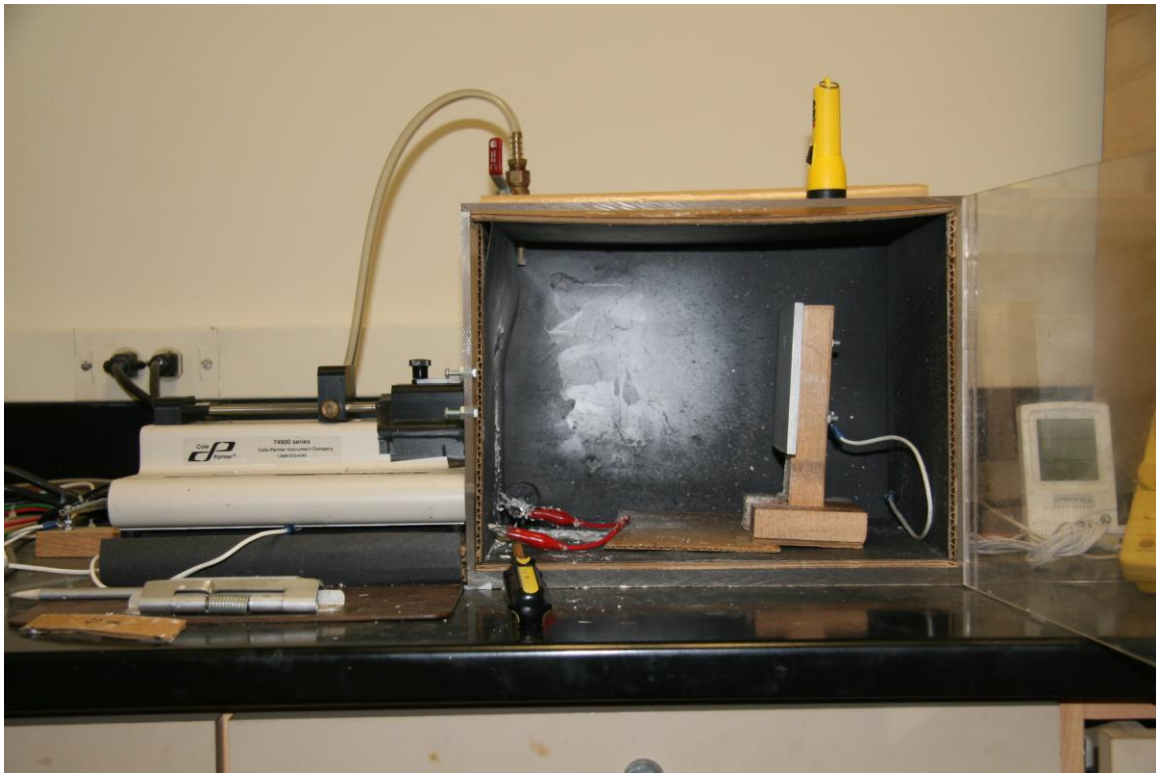

Fig. 18. Electrospinning Apparatus

6. Results

6.1 Degradation Analysis

The organotin displayed different behaviors during degradation depending upon the temperature being applied. At the lower temperatures (175 C and 200 C) the organometallic powder melted to form a clear/white liquid with many air bubbles of both large and small sizes. As time went on and the heating continued, the liquid changed to a brownish, gold color, a change most likely caused by oxidation, and the air bubbles remained. During cooling, these liquids solidified into very brittle, glassy surfaces in 10 to 30 seconds. This liquid to solid behavior continued until the sample had sufficiently degraded to the point such that it took the form of brittle, brown flakes. These flakes held their structure under heating but their color changed to dark brown by the end of the test.

Degradation at these temperatures was also very slow, taking as along as 36 hours just to achieve ~35.5% weight loss, as seen in figure 19.

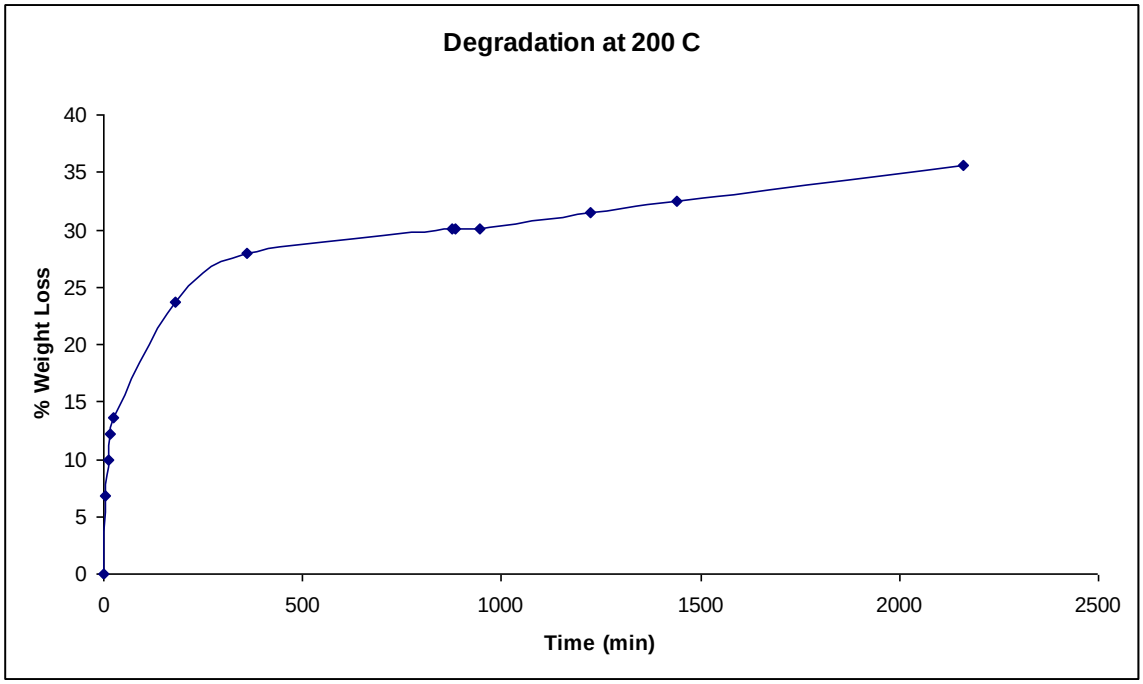

Fig. 19. Graph showing weight loss over time at 200 C

When samples were degraded at 300 C and above, degradation happened much faster than at temperatures below the melting point of tin (231 C). Peak weight loss was found to be between 41% and 48% and the time taken to reach maximum degradation was fairly consistent among all temperatures at or above 300 C as shown in Figure 20.

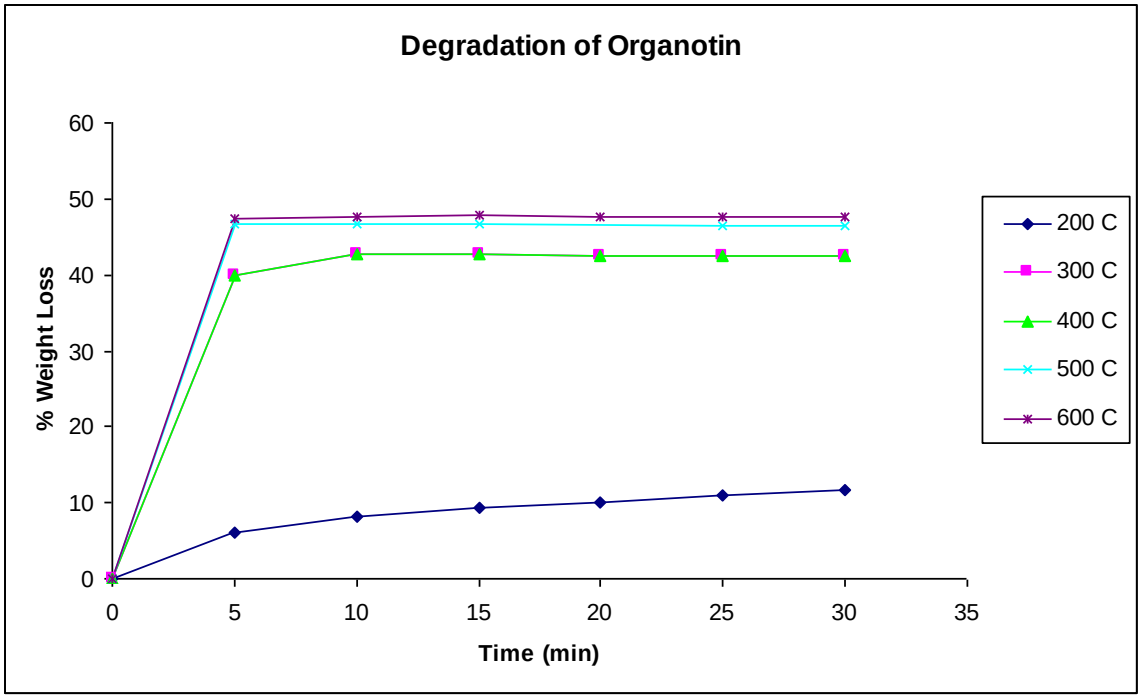

Fig. 20. Weight loss of organotin at 200 C, 300 C, 400 C, 500 C and 600 C

Degradation at these higher temperatures was also much more violent than at the lower temperatures. Instead of melting into a viscous liquid, the sample formed a brown, flaky bubble-like structure in less than 5 minutes. This was probably due to the speed of the degradation causing the air bubbles to inflate the sample in its liquid state, instead of slowly escaping over time. The sample then lost its structure and became a mix of gray and black flakes and powder, almost resembling ash. Figure 21 summarizes the degradation of the organometallic powder at different percent weight losses.

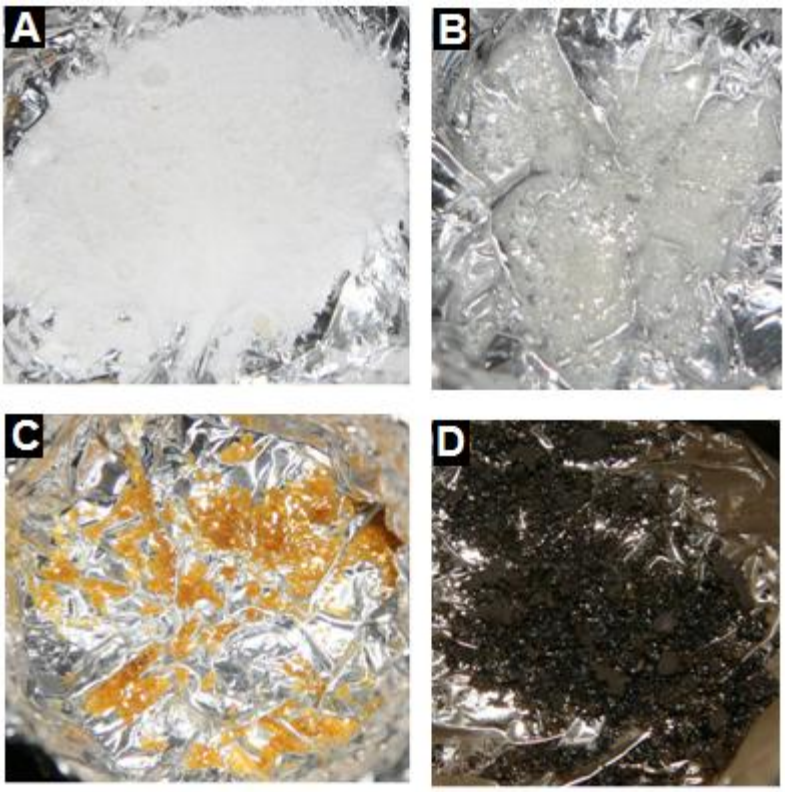

Fig. 21. (A) Organotin powder. (B) ~10% degradation. (C) ~35% degradation. (D) ~44% degradation.

The data collected and visual observations made during the degradation tests at the lower temperatures suggest that heating the electrospun organometallic at or below 200 C would be insufficient. The degradation occurs much too slowly to be acceptable if metallic fibers were to ever be manufactured with this method and material. The organometallic could not reach maximum degradation even after 36 hours of heating. The fact that the organometallic becomes liquid suggests that any fibrous structure produced during the initial electrospinning process would lose their form under heating and spread out across the surface of the aluminum foil collection plate.

300 C seemed to be the ideal temperature for degrading the samples because it allowed the organometallic to reach maximum degradation within a relatively short amount of time. Temperatures higher than 300 C also reached maximum degradation but

the samples seemed to react much more violently, as suggested by the amount of residue on the side of the aluminum cups. These violent reactions are also the likely cause of the weight loss measurements being consistently larger at the higher temperatures. These discrepancies were due to material being thrown out of the aluminum containers. Tabulated data of all weight loss tests can be viewed in the appendix.

6.1.1 Differential Scanning Calorimeter

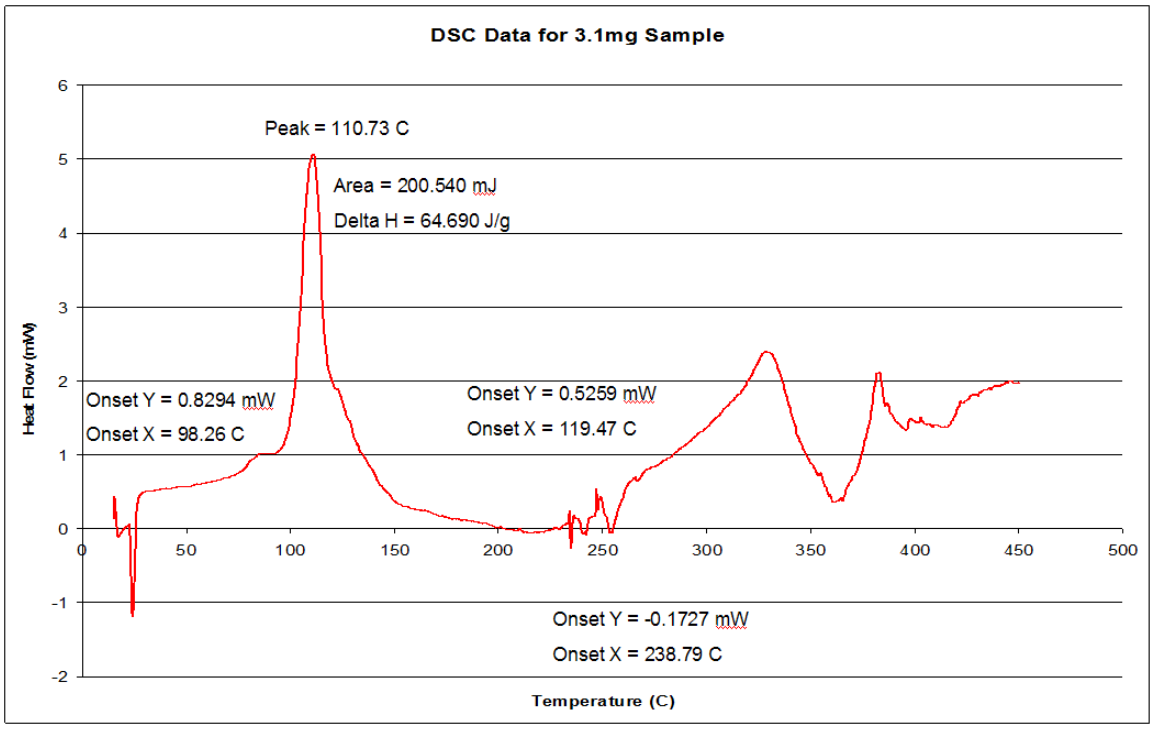

Fig. 22. DSC graph for 3.1mg sample of organotin

The DSC data in Figure 22 shows a peak at 110.73 C, which represents degradation due to water loss.

The amount of weight loss due to water evaporating can be calculated by taking the area of the peak and dividing by the delta H of water, 40.65 kJ/mol.

$$\frac{200.54 \cdot 10^{-3}\,\text{J}}{2261.11\,\frac{\text{J}}{\text{g}}} = 8.869 \times 10^{-5}\,\text{g} \qquad \frac{8.869 \times 10^{-5}\,\text{g}}{3.1 \cdot 10^{-3}\,\text{g}} \cdot 100 = 2.861$$

2.86% of the total mass loss of this sample was due to the evaporation of water.

The graph also confirms that degradation of the powder occurs between 250 C and 300 C, which corresponds to conclusions made from the previous test.

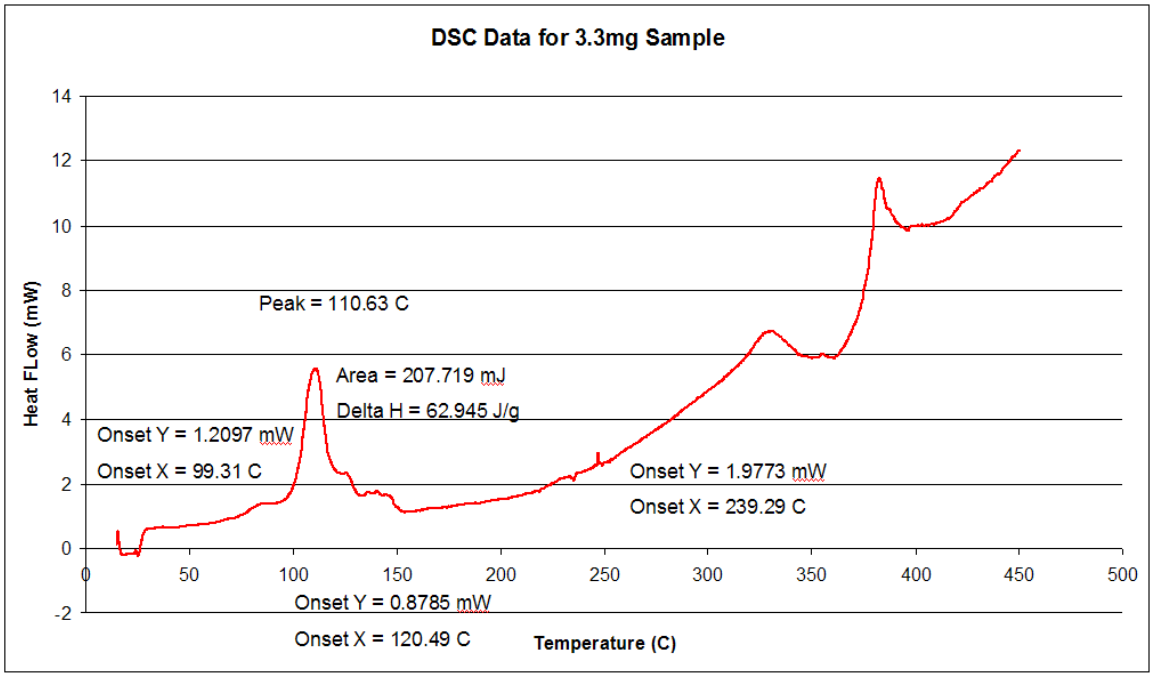

Fig. 23. DSC graph for 3.3mg sample of organotin

Similarly, mass loss due to the evaporation of water for the 3.3mg sample is calculated as:

$$\frac{207.719 \cdot 10^{-3}\,\text{J}}{2261.11\,\frac{\text{J}}{\text{g}}} = 9.187 \times 10^{-5}\,\text{g} \qquad \frac{9.187 \times 10^{-5}\,\text{g}}{3.3 \cdot 10^{-3}\,\text{g}} \cdot 100 = 2.784$$

2.78% of the total mass loss was caused by water, which closely matches the water loss from the 3.1mg sample.

The graph shows agreement with both the first DSC graph and the furnace test that degradation powder degradation begins between 250 C and 300 C.

6.1.2 X-Ray Diffraction

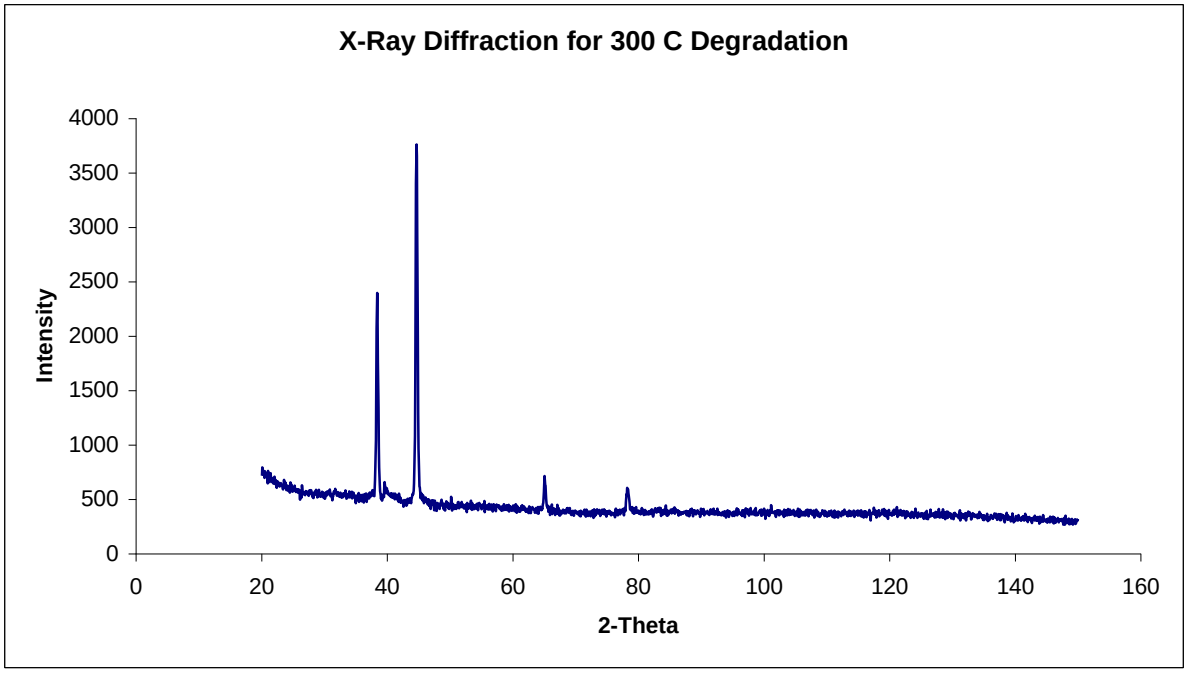

Fig. 24. XRD results for organotin sample degraded at 300 C

XRD analysis revealed only peaks for aluminum which was used to hold the degraded sample.

Since the amounts of organotin present in all of the electrospun solutions were so small, it was decided that EDS analysis would be best for determining the composition of the samples before and after degradation.

6.2 Electrospinning

Before the electrospinning could take place, the various solutions had to be prepared. Butyltin chloride dihydroxide was not soluble in water; in fact it did not even get the powder wet. Murikami et al. [20] cited ethanol as the solvent used to dissolve several different organotin compounds. Ethanol had the identical reaction as water to the

organotin chosen for this experiment. Several different organic solvents were tested including chloroform, tetrahydrofuran (THF), Dimethylformamide (DMF), and ethyl acetate. Chloroform, THF and DMF mixtures appeared to form slurries rather than solutions and most of the organometallic powder eventually precipitate out of the solvent and settled at the bottom of the mixing beaker. Ethyl acetate also formed a cloudy, slurry-like mixture but the powder did not readily precipitate out so it became the main solvent used throughout most of the electrospinning trials.

6.2.1 Solution 1 - 10% PVA (Mw 146,000 – 186,000), 20% Surfactant, and 5% Organotin

The first solution attempted to use distilled water as the solvent by using a surfactant (sodium dodecyl sulfate) to assist in the dissolution of the organotin. The resulting mixture had visible powder particles and air bubbles. The results of the first electrospinning attempt, using a 30 gauge syringe are shown in Figure 25.

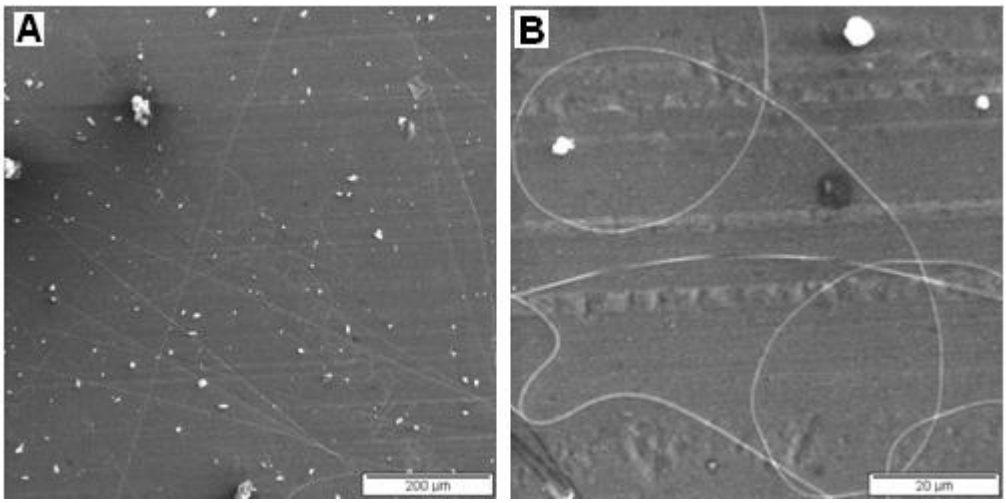

Fig. 25. SEM photographs of solution 1 electrospun through a 30 gauge needle. (A) 100x (B) 1000x

The organotin particles were too large for the needle, which resulted in clogging and very little polymer getting through. The large particles also sprayed across the surface of the collection plate instead of being contained within the polymer fibers. To help facilitate the electrospinning process, the solution was switched into a syringe with an 18 gauge needle.

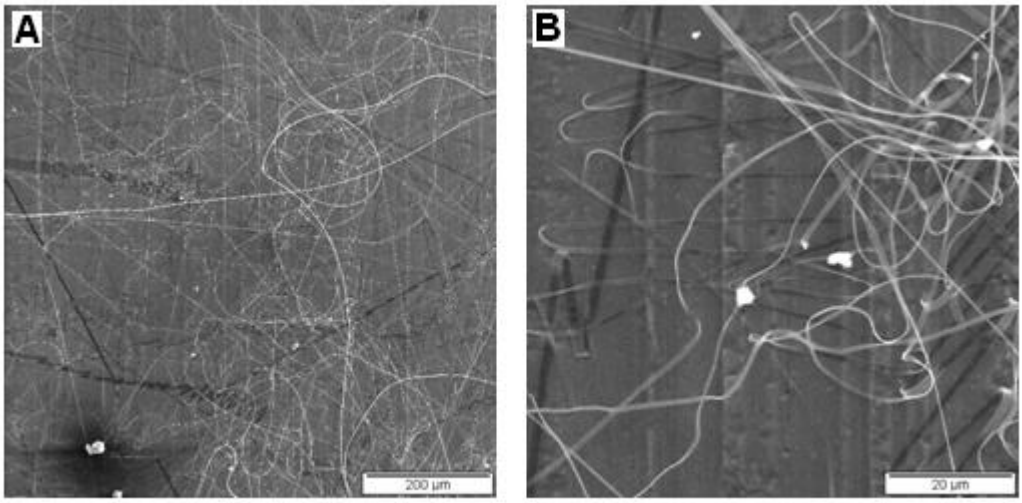

Fig. 26. SEM photographs of solution 1 electrospun through an 18 gauge needle. (A) 100x (B) 1000x

This adjustment improved the electrospinnability of this solution, as seen in Figure 26 by the significant increase in fiber density. However, the organotin can clearly be seen laying in large chunks on top of the polymer fibers, which was not the desired result and made the formation of metal or metal-oxide fibers unlikely.

6.2.2 Solution 2 - 8% PS (Mw 400,000), 2% Organotin in 1mL Ethyl Acetate

The second solution attempted to utilize the best performing solvent, ethyl acetate, in conjunction with a low concentration of organotin in hopes of making a more uniformly distributed solution. Polystyrene was chosen because it is also soluble in ethyl

acetate. SEM photographs of the electrospun structure for this solution are shown in Figure 27.

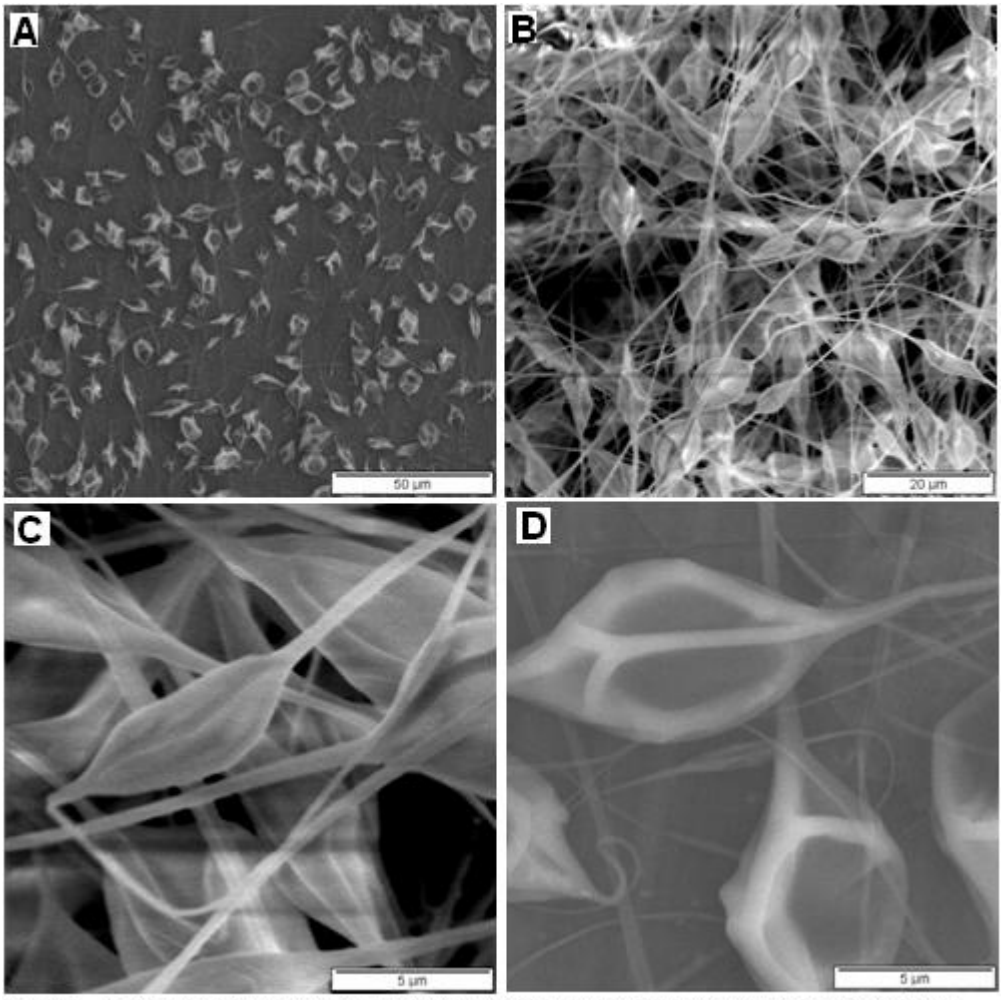

Fig. 27. SEM photographs of structures formed by electrospinning solution 2. (A) 500x (B) 1000x (C) and (D) 5000x

These structures, resembling beads connected by a string, seemed to show a potentially successful trial but upon degradation at 300 C for 15 minutes, the SEM showed the following:

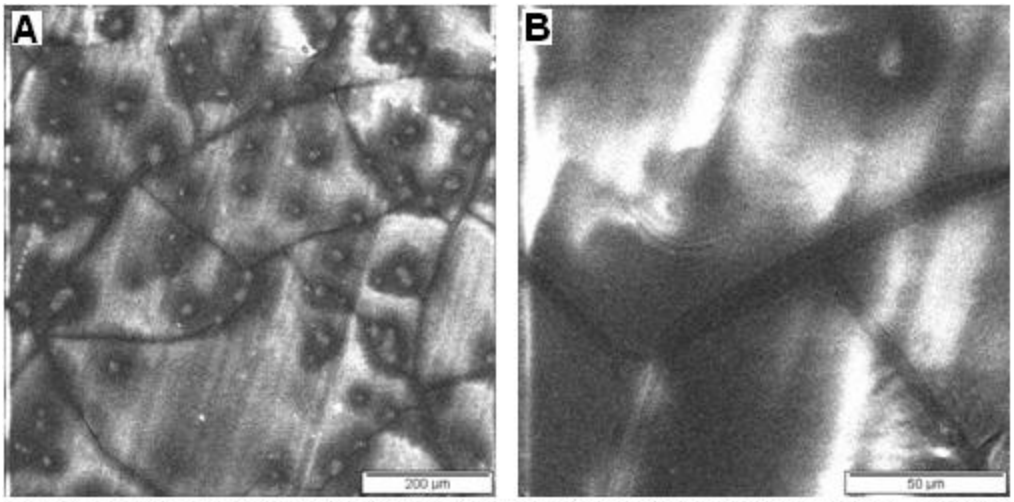

Fig. 28. SEM of carbon residue formed after degradation of fibers from solution 2. (A) 100x (B) 500x

The pictures do not clearly show the formation of any new structures, metallic or otherwise. Figures 29 and 30 show EDS data of this solution before and after degradation.

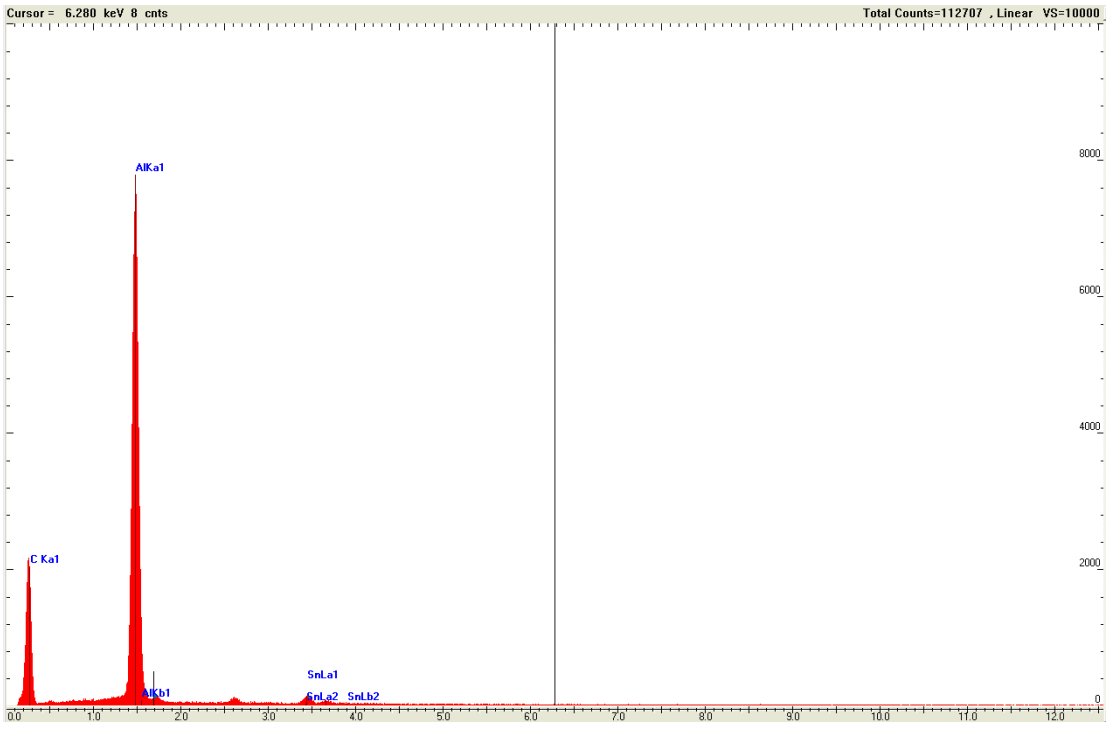

Fig. 29. EDS results from fiber from solution 2 before degradation

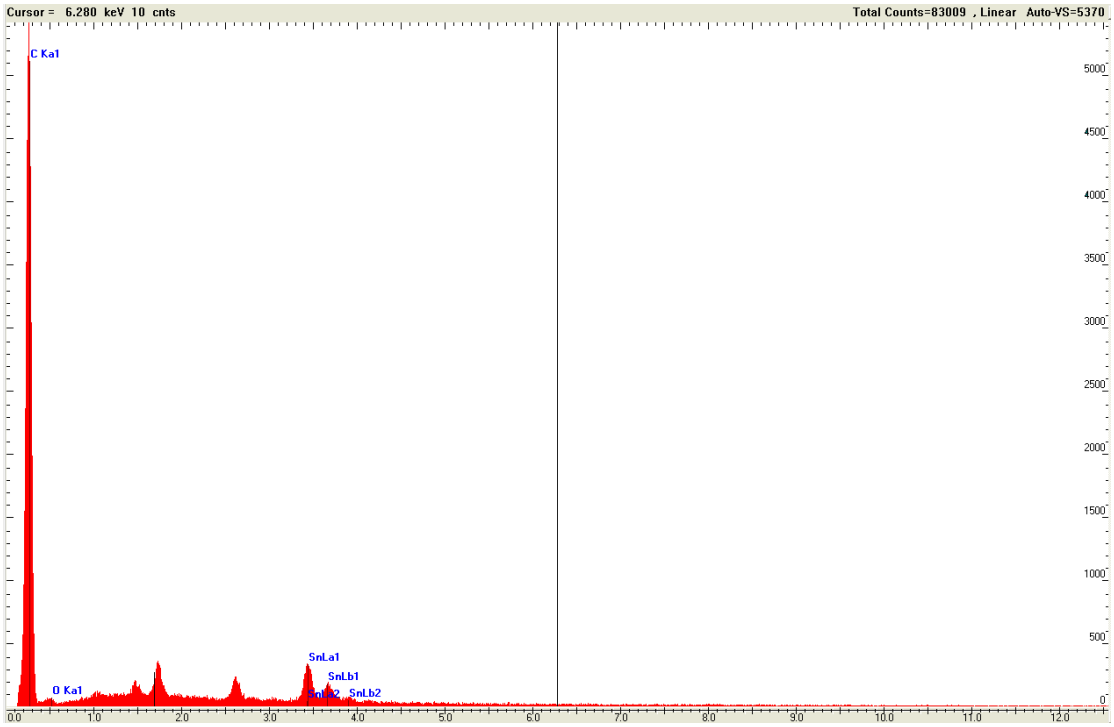

Fig. 30. EDS results of solution 2 sample after degradation

Before degradation, the scan primarily detects the aluminum background and the carbon in the polymer and the organometallic along with trace amounts of tin. After degradation, the scan detects a large amount of carbon residue covering the surface of the sample. The peaks corresponding to tin are more pronounced and there is an oxygen peak, suggesting the formation of an oxide, most likely tin oxide. The carbon residue makes detecting any tin structures on the SEM photographs impossible but the EDS does confirm that tin is present.

6.2.3 Solution 3 - 0.5% Organotin in 1mL Ethyl Acetate

This solution attempted to reduce the amount of undissolved particles in the slurry by reducing the amount of organotin and using the best solvent, ethyl acetate.

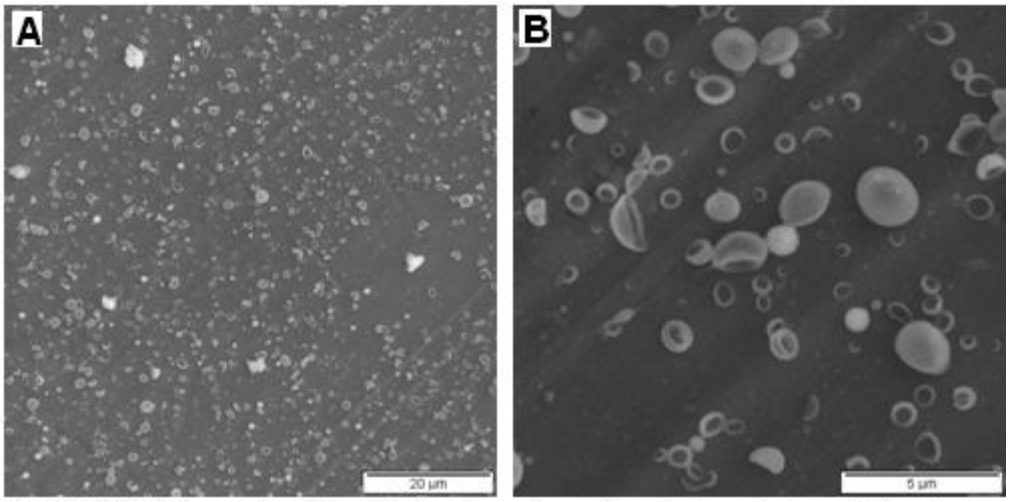

Fig. 31. SEM photographs of droplet structures formed by electrospinning solution 3. (A) 100x (B) 5000x

The mixture lacked the appropriate viscosity for electrospinning, resulting in the formation of structures resembling water droplets. While some of these droplets contain the organotin, the 100x photo clearly shows large, undissolved particles laying on the surface of the aluminum.

After the sample was degraded at 300 C for 15 minutes, the vast majority of the aluminum background was completely bare. However, on one sample, shown in Figure 32, a single structure remained.

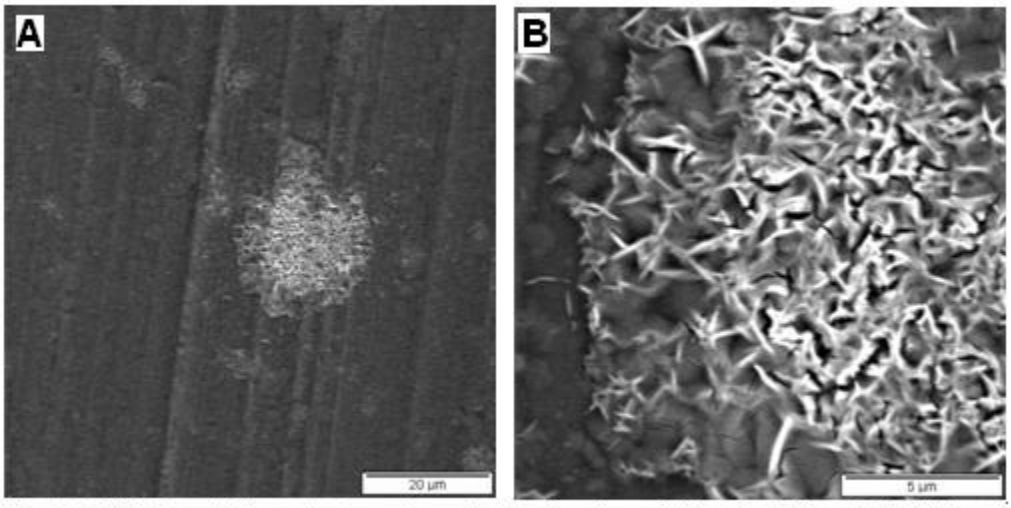

Fig. 32. SEM of crystalline structure formed after the degradation of solution 3. (A) 1000x (B)5000x

The structure shown was likely the result of a large droplet or undissolved powder particle exploding during heating and forming this crystallized residue. It appears to be a unique case as similar behavior was not seen on other parts of this sample nor was a structure like this seen on any of the other electrospun solutions.

6.2.4 Solution 4 – 2% Organotin in 0.4 HCl and 0.5 Ethanol

This mixture attempted to use hydrochloric acid to break down the organometallic compound and assist in dissolution. Ethanol was added to the organotin with no effect. The introduction of the HCl to the mixture caused the powder to completely dissolve after approximately 10 minutes of stirring. Upon electrospinning, no sample was collected on the aluminum plate. The solution may have completely evaporated when traveling between the needle and the collection plate, but the definite cause for the failure of this trial is unknown. SEM analysis showed a completely bare aluminum plate.

6.2.5 Solution 5 - 12% PS (Mw 400,000), 2% Organotin, 1mL Ethyl Acetate

According to one study, increasing the concentration of polystyrene in solution can cause the electrospun structure to transition from beads, to beads-on-a-string, and finally bead-free fibers [4]. This mixture maintained the same concentrations of organotin and ethyl acetate as in solution 2 but increased the concentration of PS by 4%. The resulting electrospun structures are show in Figure 33.

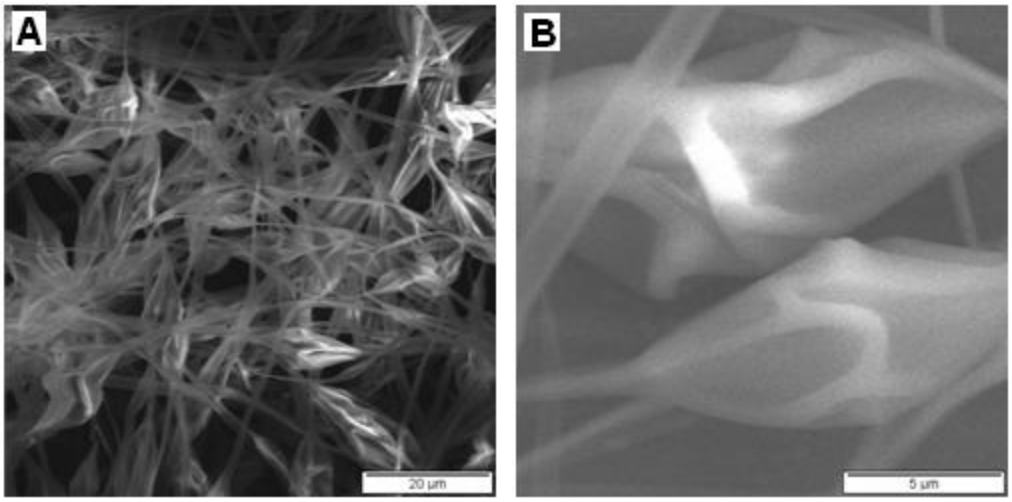

Fig. 33. SEM photographs of fibers formed by solution 5. (A) 1000x (B) 5000x

The SEM pictures show similar structures as those formed by solution 2. The beads look more elongated than those in solution 2 suggesting the transition to bead-free fibers. Degradation of this sample at 300 C for 15 minutes resulted in no observable metal or metal-oxide structures being formed.

6.2.6 Solution 6 - 5% Organotin in 1mL Ethyl Acetate

This mixture is a modification of solution 3. The concentration of organotin was increased from 0.5% to 5% in order to investigate its effect on the electrospun structure.

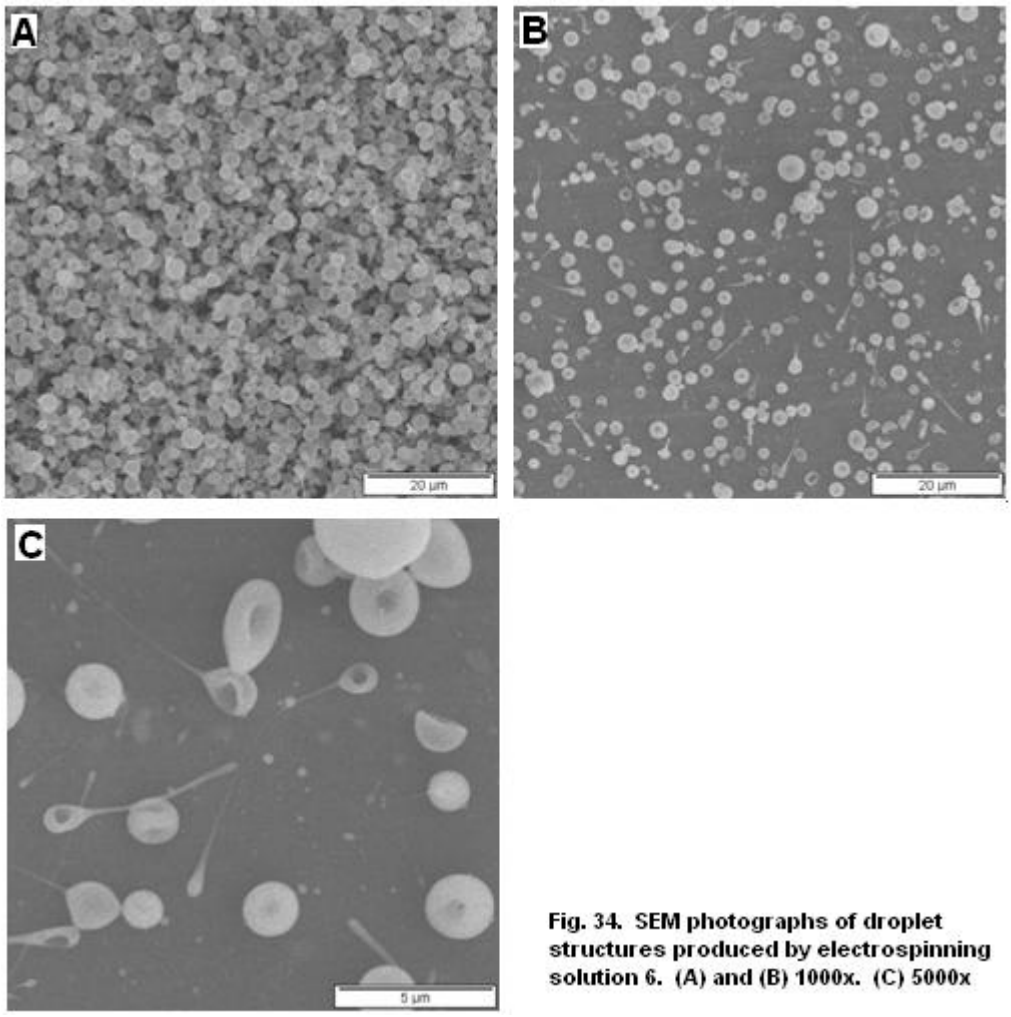

Fig. 34. SEM photographs of droplet structures produced by electrospinning solution 6. (A) and (B) 1000x. (C) 5000x

Figures 34a and 34b show that the concentration of the droplet structures increased significantly. The droplets also appear more "solid" than in solution 3, suggesting the presence of more organotin. Figures 34b and 34c also show that many of the droplets have long tails, which could mean that a transition to "beads-on-a-string" began to occur.

Degradation of this sample at 300 C for 15 minutes produced a bare aluminum surface.

6.2.7 Solution 7 - 2% Organotin in 0.2mL HCl and 1mL Dimethylformamide

This solution was another attempt at breaking down the organotin with acid and dissolving it in one of the less effective organic solvents. Upon electrospinning, this solution did not stick to the collection plate. Liquid collected and slid down the face of the aluminum. This was likely caused by the solvent not evaporating while in transit between the syringe and collection plate. Nonetheless, viable samples were still obtained from the area around where the solvent dripped.

Even before SEM analysis, small white particles of the powder were visible on the collection plate. However, they appeared much smaller than the particles seen before the solution was mixed proving the acid had effectively broken down the organotin.

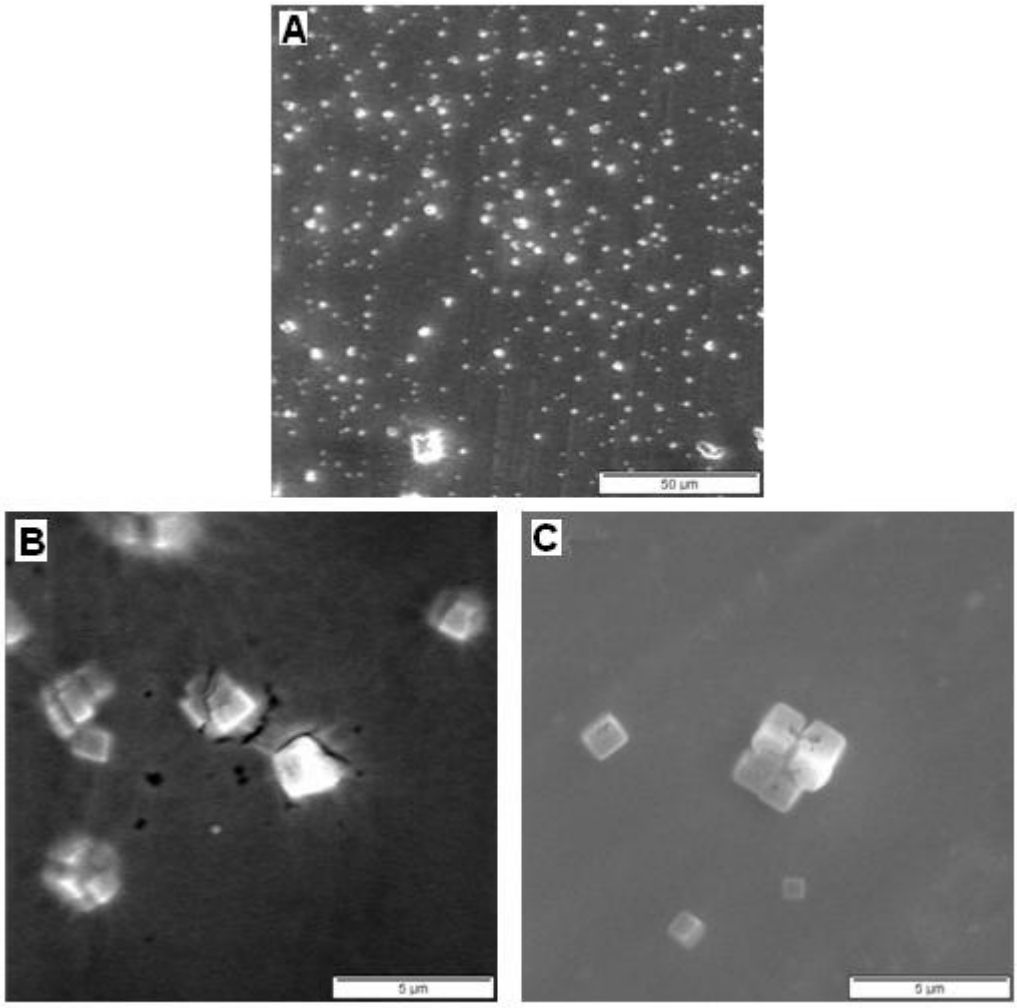

Fig. 35. SEM photographs of the cube structures formed by electrospinning solution 7. (A) 1000x. (B) and (C) 5000x

The SEM shows a series of particles with complex structures sprayed across the surface of the aluminum. These are simply small particles of the organotin powder. While this mixture was not very electrospinnable, it did show that the organometallic could be broken down into smaller particles, information that could prove useful in later studies. If these smaller particles could be combined with a polymer, a more viable mixture could result as these particles can more easily fit inside of the polymer fibers. A sufficient quantity of these organotin particles inside the polymer fiber could result in the formation of a chain of metal or metal-oxide upon degradation.

Figure 36 shows SEM photographs of solution 7 after degradation at 300 C for 15 minutes.

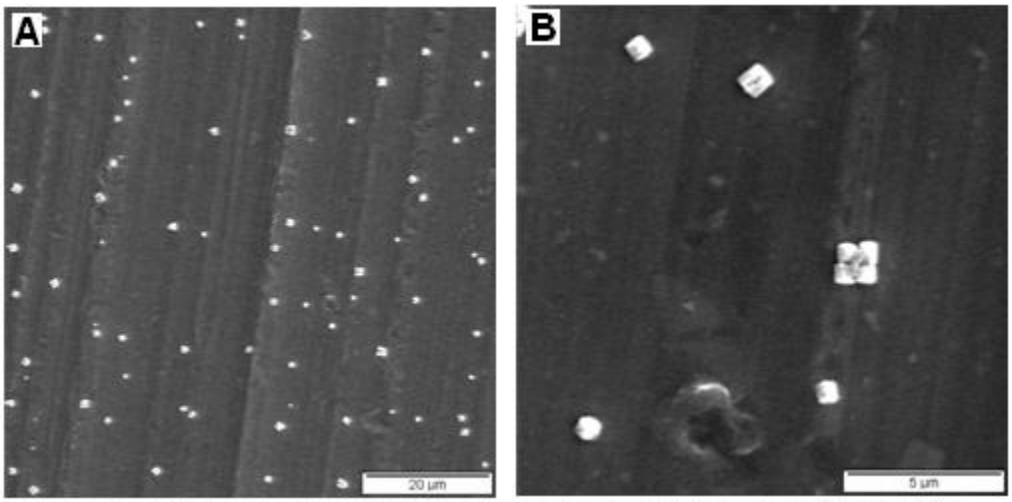

Fig. 36. SEM photographs of the degraded particles from solution 7. (A) 1000x (B) 5000x

The particles appear to have more uniform structuring and are smaller than the particles seen before degradation took place. This confirms that the organotin lost mass as intended but because the solution sprayed out of the needle instead of being extruded as a fiber, there was no opportunity for more complex structures to form.

8. Conclusion and Future Work

An organometallic that met the selection criteria was successfully chosen and analyzed. The degradation analysis showed that the peak weight loss of butyltin chloride dihydroxide was ~43% and the ideal degradation temperature was approximately 300 C. This result was confirmed by data from the differential scanning calorimeter, which also revealed that ~2.8% of total weight loss was due to the evaporation of water. Unique microstructures were produced by electrospinning different types of solutions. Polymer-based solutions showed a much higher degree of electrospinnability but left significant

carbon residue upon degradation. The solvent-based solutions showed the formation of droplet structures, which could be useful as a vehicle for applying organometallic coatings on a material. The use of acid to break down the organometallic shows promise but more trials need to be done to fully explore this option.

EDS analysis confirmed the presence of tin and tin oxide particles after thermal degradation of electrospun structures. Additives may be necessary to bind the organometallic particles together to facilitate the formation of continuous or discontinuous fibers. If an effective solvent could be found that would increase the wt% of organotin in solution to 15-20%, instead of 0.5-5, particle interaction would significantly increase, which would promote the formation of tin nanostructures.

Future research for this project should focus on solvent interactions with the organometallic rather than the degradation behavior. The formation of homogeneous solutions is vital to the electrospinning process, as seen by past successes. The possibility of alloying two or more metals by means of electrospinning organometallics with different base metals should also be examined.

References

1. Cao, Guozhong Nanostructures and Nanomaterials - Synthesis, Properties and Applications. null.

2. T. J. Sill, H. A. von Recum, *Biomaterials* **29** (2008) 1989-2006

3. T. Jarusuwannapoom, W. Hongrojjanawiwat, S. Jitjaicham, L. Wannatong, M. Nithitanakul, C. Pattamaprom, P. Koombhongse, R. Rangkupan, P. Supaphol, *European Polymer Journal* **41** (2005) 409-421

4. G. Eda, *Effects of Solution Rheology on Electrospinning of Polystyrene*, April 2006

5. Lee, Stuart M. Handbook of Composite Reinforcements (pp 364, 405-417). John Wiley & Sons.

6. M. J. Koczak, S. C. Khatri, J. E. Allison, M. G. Bader, Metal-Matrix Composites for Ground Vehicle, Aerospace and Industrial Applications

7. H. Jang, K. Ko, S.J. Kim, R.H. Basch, J.W. Fash, *Wear* **256** (2004) 406-414

8. L. Tadrist, M. Miscevic, O. Rahli, F. Topin, *Experimental Thermal and Fluid Science* **28** (2004) 193–199

9. K. M. Lee, Y. S. Lee, Y. M. Jo, J. *Air & Waste Manage. Assoc.* **56**:1139-1145

10. Kalpakjian, Serope, Manufacturing Engineering and Technology – 4th Edition. 2001, Prentice-Hall Inc, New Jersey

11. Lewis, Richard J., Sr. (2002). Hawley's Condensed Chemical Dictionary (14th Edition). John Wiley & Sons.

12 Notargiacomo, E. Giovine, F. Evangelisti, V. Foglietti, R. Leoni, *Mat. Sci. and Eng. C* **19** (2002) 185-188

13 L Bernard, M Calame, S J van der Molen, J Liao, C Schonenberger, *Nanotechnology* **18** (2007) 235202 (6pp)

14 H. Xu, D. Qin, Z. Yang, H. Li, *Materials Chemistry and Physics* **80** (2003) 524-528

15 H. Y. Dang, J. Wang, S. S. Fan, *Nanotechnology* **14** (2003) 738-741

16 M. S. Silberberg, Chemistry – The Molecular Nature of Matter and Change, 4th Edition. 1945 – McGraw Hill publishing

17 G. E. Coates, M. L. H. Green, P. Powel, K. Wade, Principles of Organometallic Chemistry. 1968 Methuen & Co. Ltd.

18 J. S. Thayer, Organometallic Chemistry, an overview. 1988 VCH Publishers, Inc. New York, NY

19 Y. Wang, M. Aponte, N. Leon, I. Ramos, R. Furlan, N. Pinto, *J. Am. Ceram. Soc*. **88** (8) 2056-2063 (2005)

20 K. Murakami, I. Yagi, S. Kaneko, *J. Am. Ceram. Soc*. **79** [10] 2557-62 (1996)

Appendix A

Data from degradation analysis

Degradation at 175 C

T = 175C	Container Wt	Total Initial Wt.	Initial Sample Wt
	2.5707	6.652	4.0813
Time	Total Weight	Sample Weight	% Wt. Loss
0	6.652	4.0813	0
60	6.2485	3.6778	9.886555754
90	6.206	3.6353	10.92789062
120	6.1651	3.5944	11.9300223
150	6.128	3.5573	12.83904638

Degradation at 175 C

T = 175C	Container Wt	Total Initial Wt.	Initial Sample Wt
	3.1934	7.619	4.4256
Time	Total Weight	Sample Weight	% Wt. Loss
0	7.619	4.4256	0
10	7.3299	4.1365	6.532447578
20	7.2476	4.0542	8.39208243
30	7.2099	4.0165	9.243944324
40	7.1802	3.9868	9.915039769
50	7.149	3.9556	10.62002892
60	7.1157	3.9223	11.37246927
90	7.0543	3.8609	12.75985177

Degradation at 200 C

T = 200C	Container Wt	Total Initial Wt.	Initial Sample Wt
	2.71	6.8666	4.1566
Time	Total Weight	Sample Weight	% Wt. Loss
0	6.8666	4.1566	0
5	6.6191	3.9091	5.954385796
10	6.527	3.817	8.170139056
15	6.4791	3.7691	9.322523216
20	6.448	3.738	10.07073089
25	6.4103	3.7003	10.97772218
30	6.3805	3.6705	11.69465428
35	6.3681	3.6581	11.99297503
40	6.3402	3.6302	12.6641967
50	6.2937	3.5837	13.78289949
60	6.2551	3.5451	14.71154309
70	6.2196	3.5096	15.56560651

Degradation at 250 C

T = 250C	Container Wt	Total Initial Wt.	Initial Sample Wt
	1.0453	1.2116	0.1663
Time	Total Weight	Sample Weight	% Wt. Loss
0	1.2116	0.1663	0
5	1.1928	0.1475	11.30487072
10	1.187	0.1417	14.7925436
15	1.1812	0.1359	18.28021648
20	1.1758	0.1305	21.52736019
25	1.169	0.1237	25.61635598
30	1.1643	0.119	28.44257366
35	1.1608	0.1155	30.54720385
45	1.1584	0.1131	31.99037883
50	1.1575	0.1122	32.53156945
60	1.1555	0.1102	33.73421527
75	1.1535	0.1082	34.93686109
90	1.1522	0.1069	35.71858088
105	1.151	0.1057	36.44016837
120	1.1493	0.104	37.46241732
150	1.1478	0.1025	38.36440168
167	1.1477	0.1024	38.42453397
182	1.1473	0.102	38.66506314
192	1.1472	0.1019	38.72519543

Degradation at 300 C

T = 300C	Container Wt	Total Initial Wt.	Initial Sample Wt
	1.1492	1.2905	0.1413
Time	Total Weight	Sample Weight	% Wt. Loss
0	1.2905	0.1413	0
5	1.234	0.0848	39.98584572
10	1.2301	0.0809	42.74593064
15	1.2301	0.0809	42.74593064
20	1.2305	0.0813	42.46284501
25	1.2305	0.0813	42.46284501
30	1.2303	0.0811	42.60438783

Degradation at 300 C

T = 300C	Container Wt	Total Initial Wt.	Initial Sample Wt
	3.153	7.3225	4.1695
Time	Total Weight	Sample Weight	% Wt. Loss
0	7.3225	4.1695	0
10	5.7525	2.5995	37.65439501
15	5.421	2.268	45.60498861
20	5.4343	2.2813	45.28600552
25	5.434	2.281	45.29320062
30	5.435	2.282	45.26921693

Degradation at 300 C

T = 300C	Container Wt.	Total Initial Wt.	Initial Sample
	1.8819	5.594	3.7121
Time	Total Weight	Sample Weight	% Wt Loss
0	5.594	3.7121	0
10	4.418	2.5361	31.68018103
20	3.9944	2.1125	43.09151154
30	3.9987	2.1168	42.97567415

Degradation at 300 C

T = 300C	Container Wt.	Total Wt.	Time	Sample Wt.	% Wt. Loss
	2.6364	3.4107	0	0.7743	0
		3.2264	5	0.59	23.80
		3.1545	10	0.5181	33.09

Degradation at 350 C

T = 350C	Container Wt.	Total Wt.	Time	Sample Wt.	% Wt. Loss
	2.2401	2.8747	0	0.6346	0
		2.5868	5	0.3467	45.37
		2.5842	10	0.3441	45.78

Degradation at 400 C

T = 400C	Container Wt	Total Initial Wt.	Initial Sample Wt
	0.8897	1.0099	0.1413
Time	Total Weight	Sample Weight	% Wt. Loss
0	1.0099	0.1413	0
5	0.9537	0.0848	39.98584572
10	0.9532	0.0809	42.74593064
15	0.9532	0.0809	42.74593064
20	0.9528	0.0813	42.46284501
25	0.9528	0.0813	42.46284501

Degradation at 400 C

T = 400C	Container Wt.	Total Wt.	Time	Sample Wt.	% Wt. Loss
	2.1028	2.896	0	0.7932	
		2.5143	5	0.4115	48.12
		2.513	10	0.4102	48.29

Degradation at 400 C

T = 400C	Container Wt.	Total Wt.	Time	Sample Wt.	% Wt. Loss
	1.8646	2.5014	0	0.6368	
		2.2053	5	0.3407	46.50
		2.2029	10	0.3383	46.88

Degradation at 500 C

T = 500C	Container Wt	Total Initial Wt.	Initial Sample Wt
	1.0999	1.191	0.0911
Time	Total Weight	Sample Weight	% Wt. Loss
0	1.191	0.0911	0
5	1.1484	0.0485	46.76180022
10	1.1484	0.0485	46.76180022
15	1.1485	0.0486	46.65203074
25	1.1487	0.0488	46.43249177

Degradation at 550 C

T = 550C	Container Wt	Total Initial Wt.	Initial Sample Wt
	1.0227	1.1555	0.1328
Time	Total Weight	Sample Weight	% Wt. Loss
0	1.1555	0.1328	0
5	1.0912	0.0685	48.4186747
10	1.091	0.0683	48.56927711
15	1.0909	0.0682	48.64457831
20	1.091	0.0683	48.56927711

Degradation at 600 C

T = 600C	Container Wt	Total Initial Wt.	Initial Sample Wt
	0.9828	1.06	0.0772
Time	Total Weight	Sample Weight	% Wt. Loss
0	1.06	0.0772	0
5	1.0235	0.0407	47.27979275
10	1.0232	0.0404	47.66839378
15	1.0231	0.0403	47.79792746
20	1.0232	0.0404	47.66839378